Proceedings of the
Annual Stability Conference
Structural Stability Research Council
San Antonio, Texas, March 19-22, 2024

A Comprehensive Approach for Estimating Residual Capacity of Damaged Steel Tubular Sections: From Surface Scanning to Stress Analysis

Prithvi Sangani[1], Smita Singh[2], and Anil Agarwal[3]

Abstract

Steel tubular sections have gained popularity in the construction industry due to their high structural efficiency and aesthetic appearance. They are extensively used in various applications, including offshore structures, power transmission poles, and industrial buildings. However, these sections can experience unexpected loads during transportation or installation, resulting in geometric defects such as dents and buckles that reduce their axial load-carrying capacity. Estimating the residual capacity of damaged steel tubular sections is vital to prevent wastage and ensure structural safety. The proposed methodology for estimating the residual capacity involved using 3D Digital Image Correlation (DIC) to scan the surface of the damaged specimen. To improve computational efficiency, the dense point cloud obtained from the surface scan was discretized into a set of coarser nodes using scattered interpolation in MATLAB. This interpolation technique utilized Delaunay triangulation to connect the scattered data points. However, polygonal-shaped specimens with abrupt changes in the unit normal at edge locations exhibited minor waviness along the edges due to the triangulation. A smoothening technique using 2D Fourier transform was employed to address this issue. The technique involved transforming the surface coordinates into Fourier transforms and applying a filter based on optimum cutoff amplitudes to smoothen the edges. By eliminating the waviness along the edges, this approach provided a better representation of the damaged tubular sections. The resulting surface mesh file was then imported into finite element software, such as ABAQUS, for stress analysis. To assess the effectiveness of the proposed method, five damaged and three undamaged specimens were analyzed using the technique to estimate their residual capacities and the results were validated through experiments, and the average estimated residual strength is about 93% of experimental results.

1. Introduction

Due to their structural efficiency, resistance against torsional buckling, and aesthetic appearance, the steel hollow tubular members have been used extensively in industrial buildings, power transmission towers, and offshore structures (Chun and Nho, 2005; Dalia et al., 2021; Duan et al., 1993; M. et al., 1994; Ricles et al., 1995; Yu and Amdahl, 2018). Tubular members are subjected to geometric defects by improper handling and heavy object impact during transportation to construction sites. It is well known that compression members are sensitive towards geometric imperfections, and hence, geometric defects can significantly lower the ultimate capacity of

[1] Research Scholar, Indian Institute of Technology, Hyderabad, India ce20resch13001@iith.ac.in
[2] Research Scholar, Indian Institute of Technology, Hyderabad, India ce17resch11007@iith.ac.in
[3] Associate Professor, Indian Institute of Technology, Hyderabad, India anil@ce.iith.ac.in

tubular columns. In such cases, estimating the residual capacity of the damaged tubular compression members becomes critical before using it for any structural applications.
Duan et al., (1993) and Ricles et al., (1995) conducted experimental studies and developed an analytical procedure to predict the behavior of damaged circular beam-columns. Salman et al., (1993) tested dent damaged circular tubular columns, developed an FE analysis to predict the moment-thrust-curvature behavior, and validated it against experiments. Prabu et al., (2010) modeled the dent as a sinusoidal shape and performed numerical analysis to compute the effect of the dent on the axial capacity of circular tubes. However, simulating the dent using FE analysis is not very practical since the shape of the indenter and the deformation applied by the indenter are unknown.

An alternate approach to measure the geometric defects involves scanning techniques to develop the full-field topographical data of the specimen. Castro et al., (2021); Humberto et al., (2021) and Ravulapalli et al., (2023) proposed a method to measure initial geometric using a simple 3D digital image correlation (DIC) setup. These studies were employed to measure the imperfections of lesser magnitude (less than 1.2mm). From the literature, it was observed that limited studies exist on damaged square tubular and exact modeling of dent shape. To address this gap, this study proposes a methodology using 3D DIC setup to scan damaged specimens. The images captured using DIC are stitched and transformed into cylindrical coordinates, and the surface point cloud data is converted to mesh after performing surface smoothing for Finite Element (FE) analysis. The resulting mesh model is analyzed to evaluate residual strength. The pictorial outline of the study is shown in Fig.1.

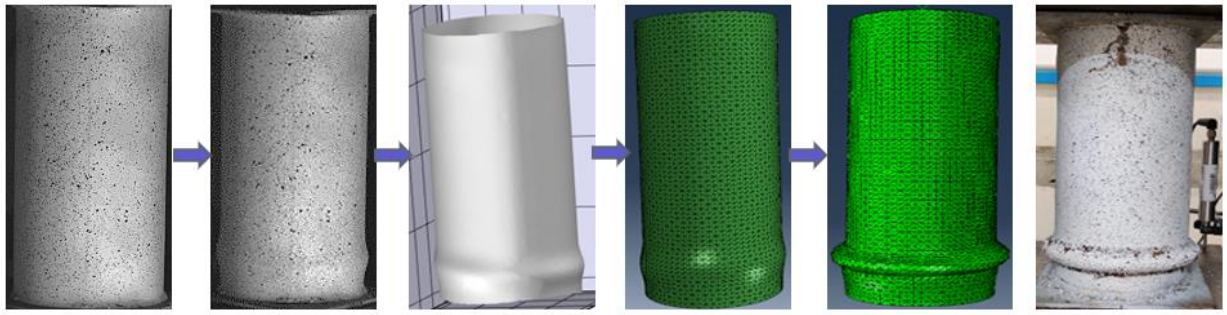

Figure 1: Outline of study

2. Work methodology

The detailed work methodology proposed to evaluate the residual strength of the damaged steel tubular columns is shown in Fig. 2. The specimen details considered for the study are presented in Table.1.

Table 1: Specimen details

Specimen Type		Size (mm)	thickness (mm)	Length (mm)	Type of Damage
Circular	C1	165	4.5	350	Undamaged/as-built, axial damage
Square	S1	220	7.6	430	Undamaged/as-built, axial damage, side dent
	S2	150	5.6	350	Undamaged/as-built, axial damage, corner dent

2.1 Experimental protocol

Three types of damages were imparted to an as-built specimen: i) axial damage: damage was introduced by compressing the as-built specimen using the compression testing machine (CTM) until a visible buckle/bulge was formed and at least 20% post-peak drop in the axial load resistance was attained (Fig.3), ii) side dent damage: damage on the square tube by pressing the cylindrical indenter (40mm Dia) along the side of the specimen at mid length, iii) corner dent damage: damage on the square tube by pressing the cylindrical indenter (40mm Dia) across the edge of the specimen at mid length on flexure testing machine (FTM). The dent depth to side ratio for both side dent and corner dent was considered as 0.1. In addition to the damaged specimen, experiments were also conducted on the undamaged as-built specimens to evaluate their axial capacity. Load values from CTM and axial strain values measured using DIC were considered to plot load vs. axial strain for each specimen. Tensile coupon tests were conducted as per ASTM E8/E8M, and the material stress-strain curves were plotted. The stress-strain plots were used for finite element analysis. After the specimen was damaged, the specimen was placed in CTM to evaluate the residual axial capacity. The load vs. axial strains of the specimen were plotted and compared with experimental results.

2.2 3D digital image correlation (DIC)

Digital Image Correlation (DIC) is a popular method used to measure surface deformations of any specimen (Correlated Solutions, Inc). In this study, DIC is used to scan the surface of the specimen. The method adopted by Castro et al., (2021); Ravulapalli et al., (2023); Sangani et al., (2023a) was used. 360^0 scanning was performed on the specimen, and the images were stitched using 3D fusion (Correlated Solutions, Inc 2023) to replicate the specimen surface. The accuracy of stitching was validated by measuring the actual dimensions of the as-built specimen. The stitched object's topographical details were extracted as a dense point cloud in terms of cartesian coordinates.

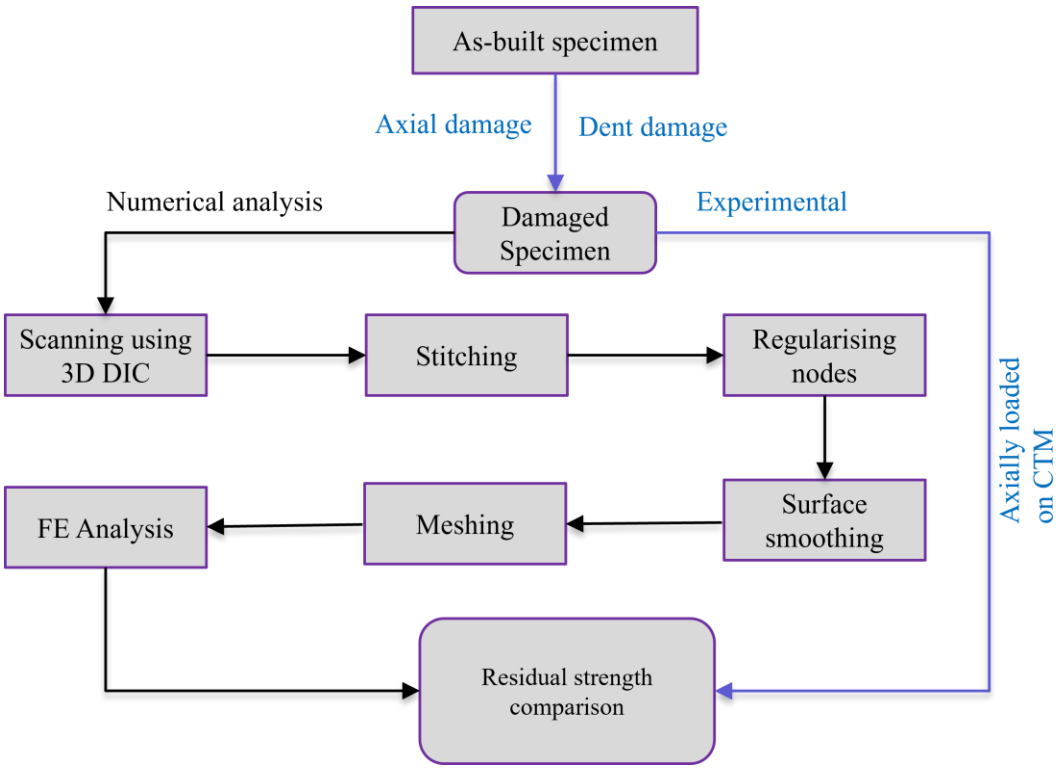

Figure 2: Work methodology

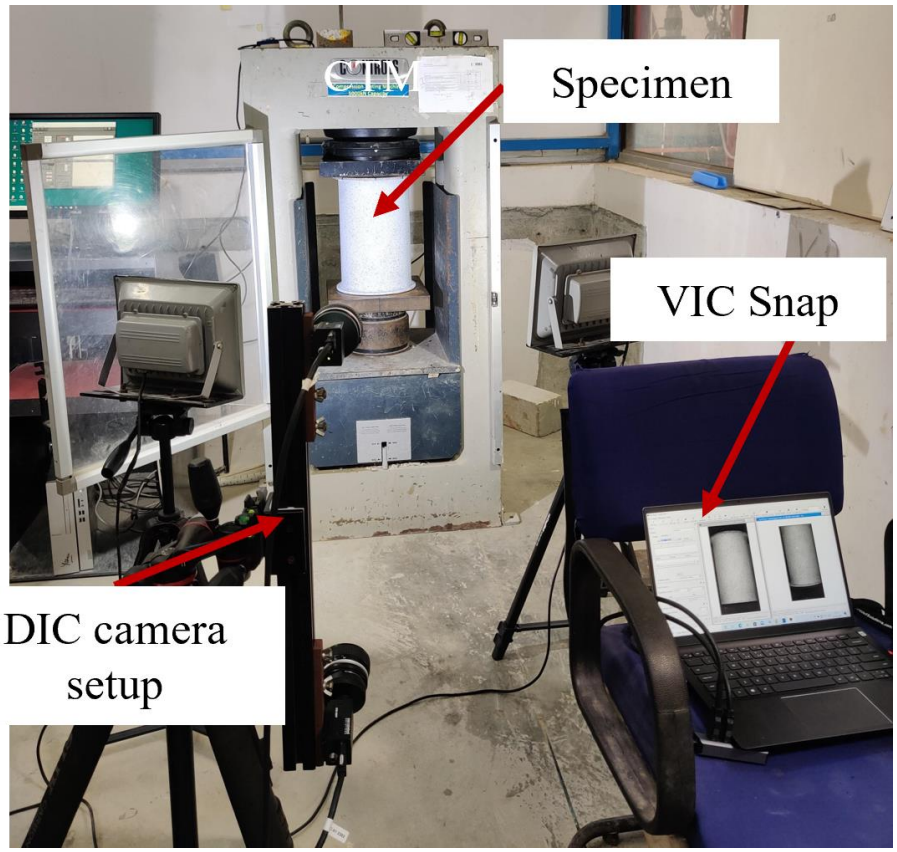

Figure 3: Experimental setup for axial damage

2.3 Processing of topographical data

The complete post-processing procedure was presented in Fig.4. The obtained surface point cloud was fine and computationally inefficient when converted to mesh for finite element analysis. The obtained data needed processing to be used for finite element analysis. The random and dense point cloud obtained were initially regularized with a user-defined node interval using Delaunay's triangulation using a scattered interpolation function (Amidror, 2002). However, a problem arises with this triangulation algorithm when it encounters a region of the model with sudden changes in the unit normal, particularly at the corners (Sangani et al., 2023b). In such cases, the interpolation results in errors, leading to the formation of wiggle patterns/undulations along the edges. These errors are the outcomes at the cost of making the mesh computationally efficient. Therefore, the challenge is to eliminate these surface undulations and unintended irregularities while smoothing the edges formed due to the interpolation function. This study proposes a 2D Fourier transform based smoothing technique for surface smoothing. The interpolated data has minor roughness/undulations, and this data can be smoothened by appropriately filtering the low-amplitude terms using the 2D Fourier transform. The filtered point cloud data replicates the damaged specimen's surface. The comparisons of specimen with no filter and after applying a filter are shown in Fig. 5. The point cloud data was imported into an open-source system software MeshLab, and the triangular meshes were generated using a Ball Pivoting Algorithm (Cignoni et al., 2018). The output file is imported as a Stereolithography (STL) file, which can be analyzed in Abaqus.

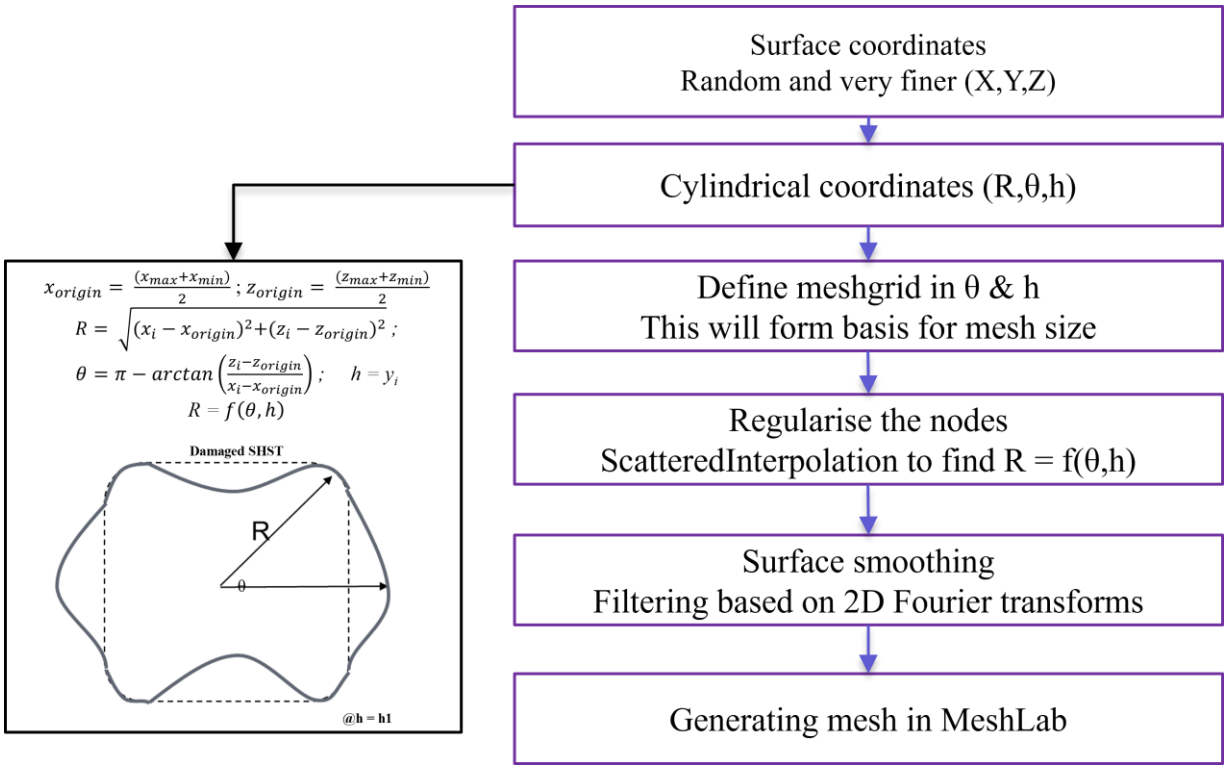

Figure 4: Processing of topographical data

2.4 Finite element analysis

The mesh was imported as an STL file after necessary smoothing and then analyzed in Abaqus. The material properties obtained from the tensile coupon test were used in the Abaqus with isotropic hardening model with Von-mises criteria. The appropriate boundary conditions were applied to the model as shown in Fig.6. Axial loading was applied and axial load vs. axial strain was evaluated and compared with experimental results.

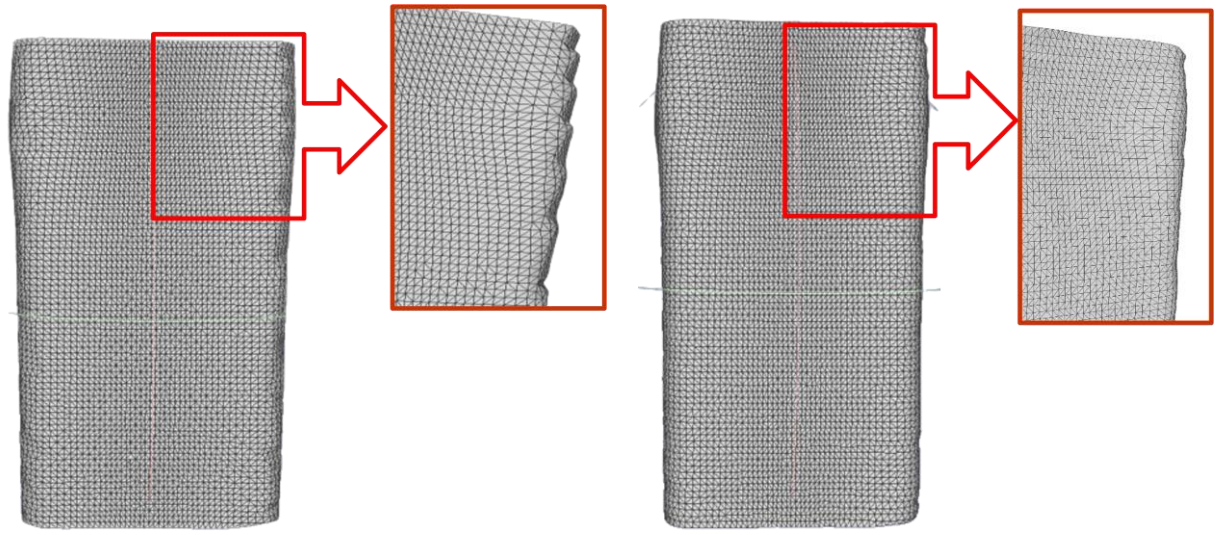

(a) Before smoothing (b) After smoothing

Figure 5: Axially damaged square tube before and after smoothing

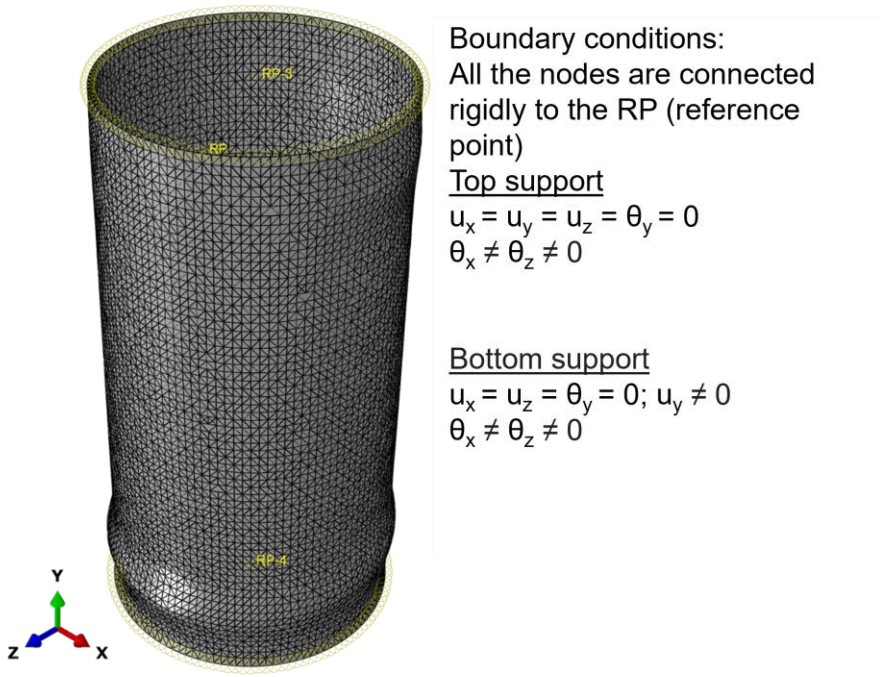

Figure 6: Scanned model of C1-axially damage along with boundary conditions

In addition to the scanned models, the models were created in Abaqus (FE models) by damaging with the same amount as in the experiment and then analyzed for residual capacity were also considered for comparisons. The ultimate loads from the scanned models (F_{scan}) and ultimate loads from the FE models (F_{model}) were compared with the experimental (F_{exp}) ultimate loads.

3. Results and discussions

Fig. 7 illustrates that the initial stiffness, ultimate loads, and strains corresponding to maximum axial loads are captured with significant accuracy in the finite element (FE) results compared to the experimental data. It was observed that the error in estimating the ultimate capacity for undamaged and axially damaged circular specimens for scanned models amounts to -3.5%, while the error in estimating using FE models amounts to 3.5%. The error in estimating the ultimate capacity for undamaged and axially damaged square specimens for scanned models amounts to -8.75%, while it is –0.75% for FE models. Likewise, the error in residual capacity estimation for the side dent damaged square specimens is -13% and -5% for scanned and FE models, respectively. While the error for corner dent damaged square specimens is about -5% and -1 %, for scanned and FE models, respectively.

The overall accuracy of the proposed method is about 93% and 100% for scanned and FE models, respectively. The overall prediction of scanned and FE model comparison with experimental results are shown in Fig. 9. Due to the presence of buckles, the induced undulations are higher in the damaged specimen than those observed in the undamaged specimen. Consequently, it can be observed that the degree of error is slightly greater in the damaged specimen when compared with the undamaged specimens. Also, it can be observed that the residual capacity for the circular specimen has an error comparatively lesser than that of the square specimen, and the same can be attributed to the presence of edges on the square specimen, which induces undulations during the process. Due to residual minor waviness along the edge after smoothing, which acts as induced local imperfections, the scanned model buckles at a load lesser than the actual load, and therefore the residual capacity of the model is expected to be comparatively lesser than the experimental residual capacity. The FE simulations effectively depict the damaged shapes compared to experimental damage modes, as demonstrated in Fig 9.

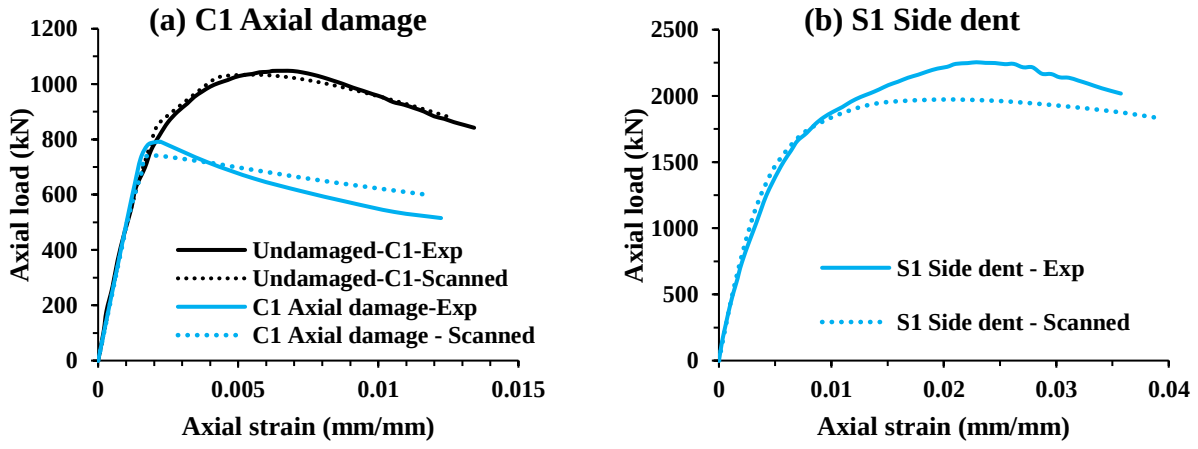

Figure 7: Comparisons of axial load vs. axial strain for experimental and scanned models

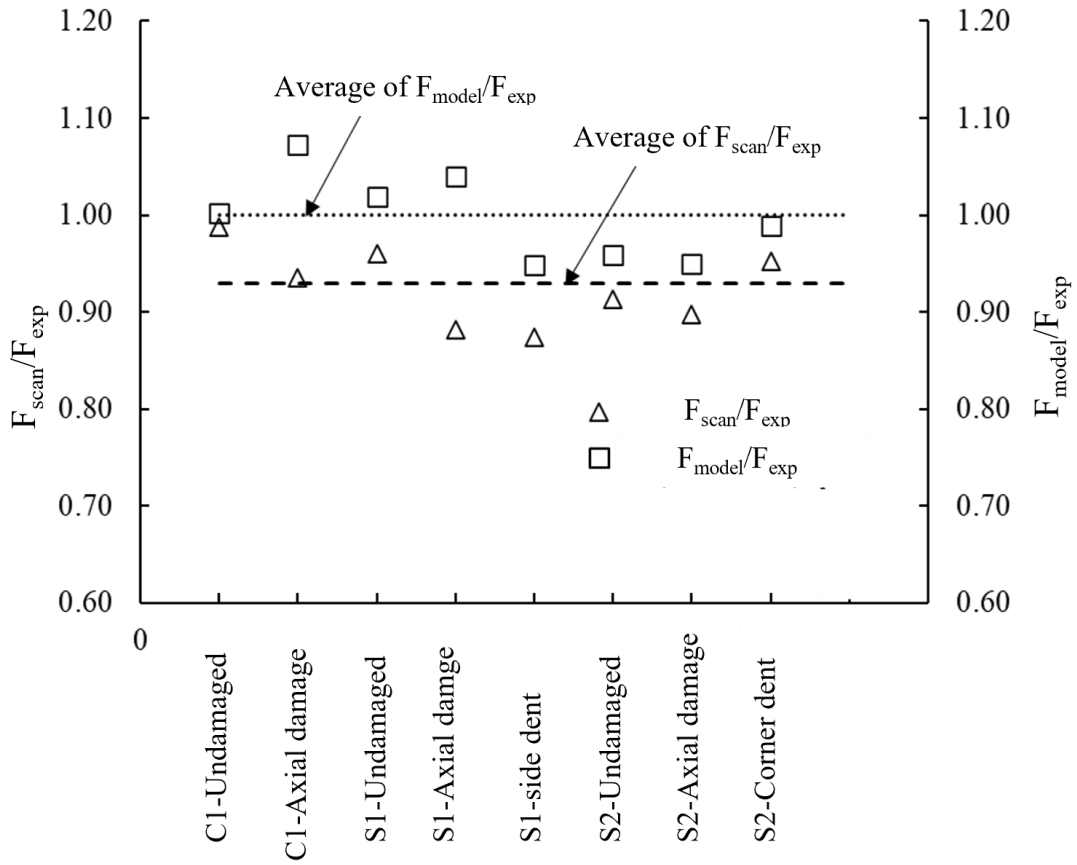

Figure 8: F_{scan}/F_{exp} and F_{model}/F_{exp} ratios for all the specimen

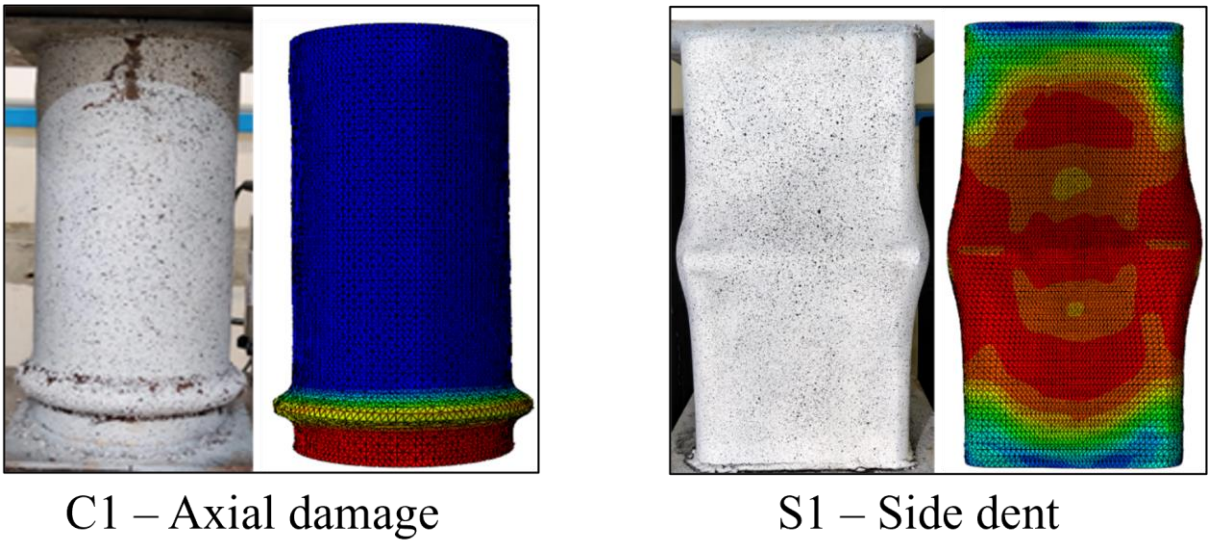

Figure 9: Comparisons of failure modes of experimental and scanned models

4. Parametric studies

For the parametric studies, the square tube was selected with 150 mm (S1) and 220 mm (S2) size. Cylindrical and spherical shapes of indenter were adopted for introducing side dent and corner dent to tubes. The diameter of the cylindrical and spherical indenter varied from 40mm to 120mm, in order to evaluate the influence of size of indentation. The length of cylindrical indenter was assumed to have higher magnitude compared to the side of the specimen such that the indentation covers entire width of the specimen. The depth to side ratio of indentation considered in experiments was 0.08 and the same ratio was considered for most of the specimens. For side dent damaged specimen with cylindrical indenter, the depth-to-side ratio was increased to 0.12 to compare the influence of depth of indentation. The FE analysis was conducted for each case and the ultimate axial loads were computed. The obtained ultimate axial loads were compared with the undamaged capacity and presented in Table. 2.

Table 2: Parametric studies for residual strength

Specimen ID	Type of damage	Shape of indenter	dia of indenter	(dent depth)/side	% residual strength
S1-S40-D008	side dent	spherical	40	0.08	79.3%
S1-S60-D008	side dent	spherical	60	0.08	79.2%
S1-S80-D008	side dent	spherical	80	0.08	78.9%
S1-S100-D008	side dent	spherical	100	0.08	78.6%
S1-S120-D008	side dent	spherical	120	0.08	78.4%
S1-C40-D008	side dent	cylindrical	40	0.08	59.9%
S1-C60-D008	side dent	cylindrical	60	0.08	59.9%
S1-C80-D008	side dent	cylindrical	80	0.08	59.8%
S1-C100-D008	side dent	cylindrical	100	0.08	59.9%
S1-C120-D008	side dent	cylindrical	120	0.08	59.7%
S1-C40-D012	side dent	cylindrical	40	0.12	52.5%
S1-C60-D012	side dent	cylindrical	60	0.12	52.9%
S1-C80-D012	side dent	cylindrical	80	0.12	53.2%
S1-C40-D004	side dent	cylindrical	40	0.04	70.9%
S1-C80-D004	side dent	cylindrical	80	0.04	71.1%
S1-C120-D004	side dent	cylindrical	120	0.04	70.4%
S2-C40-D008	corner dent	cylindrical	40	0.08	95.2%
S2-C60-D008	corner dent	cylindrical	60	0.08	95.5%
S2-C80-D008	corner dent	cylindrical	80	0.08	95.3%
S2-C100-D008	corner dent	cylindrical	100	0.08	94.8%
S2-C120-D008	corner dent	cylindrical	120	0.08	94.4%
S2-C40-D008	corner dent	spherical	40	0.08	96.3%
S2-C60-D008	corner dent	spherical	60	0.08	95.7%
S2-C80-D008	corner dent	spherical	80	0.08	95.2%
S2-C100-D008	corner dent	spherical	100	0.08	94.7%
S2-C120-D008	corner dent	spherical	120	0.08	94.3%

From the parametric studies, it was observed that side dent damaged specimens will have higher influence on residual strength compared to corner dent damaged specimens. The shape of the indenter has a lesser significance on residual strength for a corner dent damaged specimen. In contrast, the cylindrical shaped indenter lowers the residual strength of side dent damaged specimen compared to that of the spherical indenter. When the depth of indentation was increased by 50%, the residual strength of side dent damaged specimens decreased by about 7%. In all the cases, it was observed that the size of the indenter has a marginal effect on the residual strength.

5. Conclusions

The paper proposes an effective approach for predicting the residual capacity of both undamaged (3 specimens) and damaged (5 specimens) tubular columns. The accuracy of estimation is about 93% for scanned specimens. The developed model allows finite element analysis by incorporating material properties for evaluating residual capacity. The study proposes adopting material properties from initial coupon results for damaged scanned specimen. Notably, results from the scanned specimen are observed to be conservative, providing an extra margin of safety, crucial in applications prioritizing safety and reliability. For future research, the methodology can be extended to explore residual capacity of post-fire damage by integrating damaged material properties into the FE analysis. A limitation of the methodology is the inability to model solid elements, given that the elements are created by extracting surface coordinates and meshed as an STL file, containing triangular shell elements.

Acknowledgments

The first author would like to acknowledge Prime Minister's Research Fellowship (ID: 2002196), MoE, India, during this research. The authors would like to appreciate the help from Mr. Ayush in conducting parametric studies. The authors would like to acknowledge the support provided by Mr. Abhishek and Mr. Raviprakash of Pyrodynamics, India, during the 3D-DIC set up.

References

ABAQUS, ABAQUS/Standard User's Manual Volumes I-III and ABAQUS CAE Manual, Dassault Systems Simulia Corporation, 2016.

Amidror, I., 2002. Scattered data interpolation methods for electronic imaging systems: a survey. J. Electron. Imaging 11, 157. https://doi.org/10.1117/1.1455013

ASTM Standard E8/E8M, Standard Test Methods for Tension Testing of Metallic Materials, ASTM International, West Conshohocken. USA, 2011

Castro, S.G.P., Almeida, J.H.S., St-Pierre, L., Wang, Z., 2021a. Measuring geometric imperfections of variable–angle filament–wound cylinders with a simple digital image correlation setup. Compos. Struct. 276. https://doi.org/10.1016/j.compstruct.2021.11449.

Chun, T.B., Nho, I.S., 2005. Ultimate Strength Analysis of Dented Tubular Members. Fifteenth Int. Offshore Polar Eng. Conf.

Correlated Solutions Inc., VIC 3D DIC manual, 2023, http://www.correlatedsoluions.com/supportcontent/Vic-3D-9.4-Manual.pdf

Correlated Solutions Inc., Cylinder data with Vic-3D, procedure guide, 2023.

Dalia, Z.M., Bhowmick, A.K., Grondin, G.Y., 2021. Local buckling of multi-sided steel tube sections under axial compression and bending. J. Constr. Steel Res. 186. https://doi.org/10.1016/j.jcsr.2021.106909

Duan, L., Chen, W.F., Loh, J.T., 1993. Analysis of dented tubular members using moment curvature approach. Thin-Walled Struct. 15, 15–41. https://doi.org/10.1016/0263-8231(93)90011-X

José Humberto S. Almeida, Luc St-Pierre, Zhihua Wang, Marcelo L. Ribeiro, Volnei Tita, Sandro C. Amico, Saullo G.P. Castro, Design, modeling, optimization, manufacturing and testing of variable-angle filament-wound cylinders, Composites Part B: Engineering, 225, 2021, , https://doi.org/10.1016/j.compositesb.2021.109224.

M., R.J., E., G.T., William, L., 1994. Grout Repair of Dented Offshore Tubular Bracing—Experimental Behavior. J. Struct. Eng. 120, 2086–2107. https://doi.org/10.1061/(ASCE)0733-9445(1994)120:7(2086)
Ma, J.-L., Chan, T.-M., Young, B., 2016. Experimental Investigation on Stub-Column Behavior of Cold-Formed High-Strength Steel Tubular Sections. J. Struct. Eng. 142. https://doi.org/10.1061/(asce)st.1943-541x.0001456
MATLAB (2020) R2020a 9.8.0.1538580.
P. Cignoni, M. Callieri, M. Corsini, M. Dellepiane, F. Ganovelli, G.R., 2008. MeshLab: an Open-Source Mesh Processing Tool, in: Sixth Eurographics Italian Chapter Conference. pp. 129–136.
Prabu, B., Raviprakash, A. V., Venkatraman, A., 2010. Parametric study on buckling behaviour of dented short carbon steel cylindrical shell subjected to uniform axial compression. Thin-Walled Struct. 48, 639–649. https://doi.org/10.1016/j.tws.2010.02.009
Ravulapalli, V., Raju, G., Narayanamurthy, V., 2023. Experimental and numerical studies on the elasto-plastic buckling response of cylindrical shells with spigot support under axial compression. Thin-Walled Struct. 191. https://doi.org/10.1016/j.tws.2023.111095
Ricles, J.M., Bruin, W.M., Sooi, T.K., Hebor, M.F., Schonwetter, P.C., 1995. Residual Strength Assessment and Repair of Damaged Offshore Tubulars. Offshore Technol. Conf. https://doi.org/10.4043/7807-MS
Salman, W. A., Birkemoe, P. C., and Ricles, J.M., 1993. Strength assessment and repair of damaged bracing in offshore platforms, in: Annual Tech. Session and Meeting, Structural Stability Research Council, Lehigh Univ. pp. 247–258.
Sangani, P., Singh, S., Agarwal, A., 2023a. Residual Strength Estimation of Damaged Steel Tubular Columns using Digital Image Correlation. Mater. Today Proc. https://doi.org/10.1016/j.matpr.2023.11.049
Sangani P., Singh, S., Agarwal, A., 2023b "Challenges in Modeling Damaged Steel Tubular Columns for Residual Capacity Estimation. "12th International Symposium on Steel Structures, Jeju, Korea
Wardenier, J., 2011. Hollow Sections In Structural Applications, 2nd Edition, CIDECT,Geneva. 2nd Edition, CIDECT, Geneva. https://doi.org/10.1007/978-94-011-5856-5_6
Yu, Z., Amdahl, J., 2018. A review of structural responses and design of offshore tubular structures subjected to ship impacts. Ocean Eng. 154, 177–203. https://doi.org/10.1016/j.oceaneng.2018.02.009